A Radio Frequency Comb Filter for Sparse Fourier Transform-based Spectrum Sensing

Ruochen Lu, Tomás Manzaneque, Yansong Yang, Jin Zhou, Haitham Hassanieh, and Songbin Gong
Department of Electrical and Computer Engineering
University of Illinois at Urbana-Champaign, Urbana, IL
rlu10, tmanzane, yyang165, jinzhou, haitham, songbin@illinois.edu

Abstract— This work demonstrates a passive low-insertionloss (IL) RF filter with periodic passbands and capable of sparsifying the spectrum from 238 to 526 MHz for sparse Fourier transform (SFT) based spectrum sensing. The demonstrated periodic filter employs LiNbO3 lateral overtone bulk acoustic resonators (LOBARs) with high-quality factors (Qs), large electromechanical coupling (k_t^2) , and multiple equally spaced resonances in a ladder topology. The fabricated LOBARs show k_t^2 larger than 1.5% and figure of merits $(k_t^2 \cdot O)$ more than 30 for over 10 tones simultaneously and are both among the highest demonstrated in overmoded resonators. The multi-band filter centered at 370 MHz have then been obtained with a passband span of 291 MHz, a spectral spacing of 22 MHz, an IL of 2 dB, FBWs around 0.6%, and a sparsification ratio between 7 and 15. An out-of-band rejection around 25 dB has also been achieved for more than 14 bands. The great performance demonstrated by the RF filter with 14 useable periodic passbands will serve to enable future sparse Fourier transformbased spectrum sensing.

Keywords—RF filter, sparse Fourier transform, lithium niobate, piezoelectricity, lateral overtone bulk acoustic resonator

I. INTRODUCTION

In recent years, the tremendous growth of wireless applications requires better spectrum access paradigms for efficient utilization of the radio frequency (RF) spectrum. One promising approach is to use a multi-frequency dynamic spectrum access scheme, where the users can sense the spectrum in real time and then communicate within the identified idle channels [1]. In such a scenario, a real-time wide-band spectrum sensing system is the key [2], [3]. However, conventional spectrum sensing solutions that use high-speed analog to digital converters (ADCs) to sample the wide bandwidth spectrum are typically power-hungry and are thus inapt for many emerging low-power wireless applications [4]. Recently, alternative spectrum sensing approaches using sparse Fourier transform (SFT) and moderate-speed ADCs to sample at a sub-Nyquist rate [5] have been reported with low power consumption. Despite their promising prospects, these approaches can only be applied to a sparse spectrum [6], which is rarely the case for the crowded sub-GHz spectrum in urban areas. In order to exploit the benefits of SFT for sensing the majority of the sub-GHz spectrum, one method is to sparsify the spectrum in a periodic multiplexing scheme (Fig. 1) before an SFT engine is engaged for analysis. The core innovation of the scheme in Fig. 1 is the chip-scale passive RF filters with periodic passbands (i.e., comb filters) that can realize the sparsification of the spectrum. These filters should attain a sufficient number of passbands with equal frequency spacing and span a wide frequency range

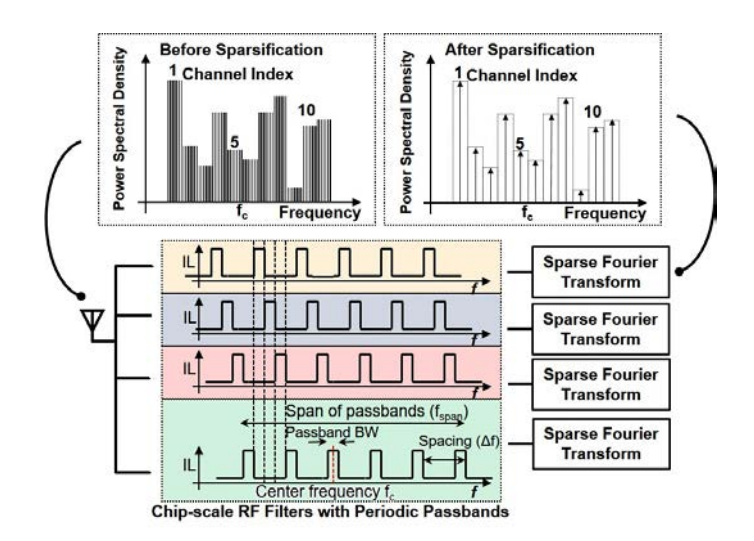


Fig. 1. Block diagram of an energy-efficient spectrum sensing front-end, consisting of a passive RF filter with periodic passband, reconfigurable RF circuits for sparsification. Multiple filters are used to sense the whole spectrum seamlessly, simultaneously, and constantly. The output signals are used for sparse Fourier transform.

to capture all relevant channels. Moreover, they should feature a suitable sparsification ratio, γ (frequency spacing over passband bandwidth), to avoid missing any occupancy information while suppressing other subsets of the spectrum outside the passbands. These requirements are extremely challenging for conventional chip-scale RF filter technologies [7]–[10] because they are optimized to couple into a single mode for producing a single passband with sufficient factional bandwidth.

In this work, we aim to demonstrate a passive low insertion loss (IL) RF comb filter based on the piezoelectric overtone resonators that have an assortment of equally spaced resonances due to the harmonic nature of a single resonant cavity. Overtone resonators have been explored in the past for attaining very high Qs in multiple piezoelectric platforms, including aluminum nitride(AlN) [11] and AlN-on-diamond [12], and lithium niobate (LiNbO₃) [13], AlN-on-SiC [14], and AlN-on-sapphire [15]. However, these past demonstrations usually have moderate electromechanical coupling, k_t^2 , which prevents these technologies from synthesizing passbands over an adequate span and with a sufficiently low IL for each passband. Recently, LiNbO₃ lateral overtone bulk acoustic resonators LOBARs based on the shear horizontal modes (SH0) has been shown with high k_t^2 $(\sim 2\%)$ and Q (>2000) simultaneously for multiple equallyspaced resonances [16]. Such high coupling and low damping

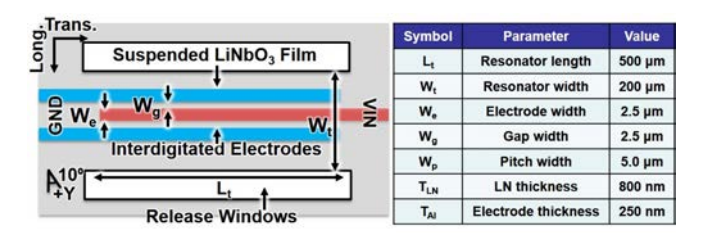


Fig. 2. Schematic of a LiNbO $_3$ LOBAR with key design parameters. A set of typical values is listed in the inset table.

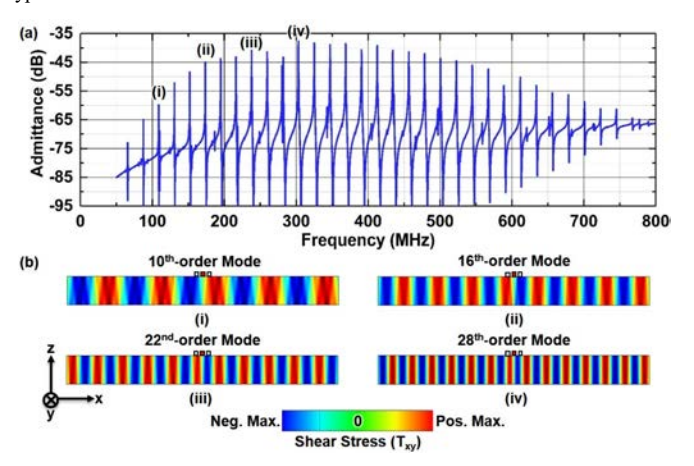


Fig. 3. (a) FEA simulated admittance response of a LOBAR with key parameters listed in the inset table in Fig. 2. (b) Simulated shear stress (T_{xy}) mode shapes for various order SH0 resonances over a wide frequency range.

characteristics in the LiNbO₃ piezoelectric platform are promising for constructing a comb filter. This work exploits the SH0 LiNbO₃ LOBARs to demonstrate a passive low-IL RF filter with periodic passbands for SFT-based spectrum sensing.

II. DESIGN AND ANALYSIS

As shown in Fig. 2, the designed SH0 LOBAR consists of a suspended LiNbO3 thin film partially covered by the interdigitated transducers (IDT). The device is oriented at -10° to +Yaxis in the X-cut plane of LiNbO₃ for exciting SH0 modes with high k_t^2 [17]. The resonator is mechanically fixed at the two ends in the transverse direction and is mechanically free at the etched edges in the lateral direction. Each IDT introduces electrical fields between its electrodes, which subsequently excite strain and stress standing waves inside the resonator cavity. Key parameters of a typical LiNbO₃ LOBAR employing 2 transducers (3 electrodes) are listed in the inset table of Fig. 2. The resonator width is significantly larger than the transducer pitch and gap width between electrodes. The admittance response of the LOBAR with its parameters in the inset table of Fig. 2 is simulated using 3-dimensional finite element analysis (FEA) in Coventorware [Fig. 3(a)]. Compared to a conventional piezoelectric resonator that targets the prominent excitation of a single mode, LOBARs support the excitation of a number of spectrally equally-spaced resonant modes simultaneously. As shown in Fig. 3(b), the FEA produced stress mode shapes (shear stress T_{xy}) at the resonance indicate that these modes are SH0 of different mode orders in the lateral direction. For avoiding ambiguity, these modes are distinguished from each other by

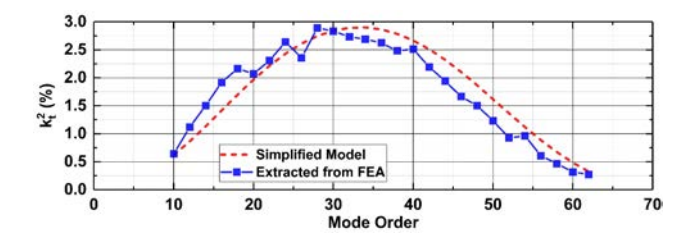


Fig. 4. k_t^2 of various even-order modes attained using the simplified model and FEA. The device dimensions are shown in the inset table in Fig. 2.

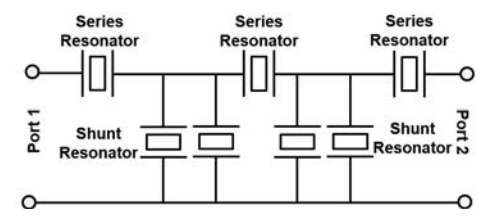


Fig. 5. Ladder filter topology consisting of 3 series resonators and 4 shunt resonators. The shunt resonators are grouped into 2 pairs.

their lateral mode orders (m), which are the numbers of displacement nodes/nulls in the lateral direction.

To design LOBARs for comb filtering, capturing k_t^2 distribution among different tones is crucial. To avoid time-consuming FEA and understand the k_t^2 distribution, we develop a simplified model based on Berlincourt formula. It describes the device transduction efficiency (k_t^2) in converting electrical energy to mechanical energy via piezoelectricity by [18]:

$$k_t^2 = \frac{U_m^2}{U_e U_d} = \frac{(\int T : d \cdot E dV)^2}{\int T : s^E : T dV \cdot \int E \cdot \epsilon^T \cdot E dV}$$
(1)

where U_m is the mutual energy, U_e is the elastic energy, and U_d is the electric energy. T is the stress tensor, and E is the electric field. d, s^E and ϵ^T denote the piezoelectric strain constants, compliance constants at a constant electric field, and permittivity constants at a constant stress respectively. Solving the equation for the cross-section of an SH0 resonator (dimensions labeled in Fig. 2) with the plane wave assumption, the results are shown in Fig. 4. The calculated results match the FEA results well.

Based on the LOBARs above, ladder filters are constructed. The advantages of a ladder topology include effective exploitation of k_t^2 for large fractional bandwidth, simple routing, and high out-of-band rejection. The circuit schematic of the designed ladder filter is shown in Fig. 5, consisting of 3 series resonators and 4 shunt resonators (grouped in 2 pairs). To create passbands, the series resonances (f_s^s) of the series resonators should be slightly offset from the series resonances (f_p^s) of the parallel/shunt resonators. The frequency offset is typically smaller than the maximum allowed FBW of the ladder topology (roughly $k_t^2/2$), and the obtained FBW is set by the resonances of the series and shunt resonators, as:

$$FBW = \frac{2(f_s^s - f_p^s)}{f_s^s + f_p^s} \tag{2}$$

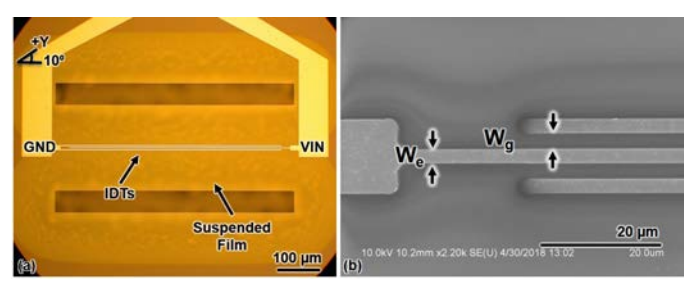


Fig. 6. (a) Optical and (b) SEM images of the fabricated LOBAR.

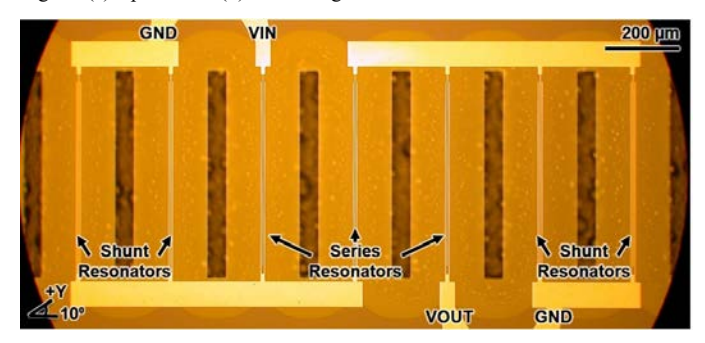


Fig. 7. Optical image of the fabricated LOBAR filter.

Thus, accurately setting the resonances of both resonators for multiple modes is essential for designing our ladder filters with periodic passbands. To this end, we choose to lithographically set the lateral dimensions (W_t) of the series and shunt resonators slightly differently. In order to have roughly the same multimode performance with comparable k_t^2 for various order modes, other design parameters of the series and shunt resonators are kept identical. The FBW can be derived as:

$$FBW = \frac{2(1/W_{t_{series}} - 1/W_{t_{shunt}})}{1/W_{t_{shunt}} + 1/W_{t_{series}}} \approx \Delta W_t/W_t$$
 (3)

where W_{tshunt} and $W_{tseries}$ are the resonator widths of the shunt and series resonators respectively. ΔW_t is the width difference. The equation is valid as long as the FBW is less than the maximum allowed value determined by the piezoelectric platform (around $k_t^2/2$ for platforms with moderate k_t^2).

III. MEASUREMENT AND DISCUSSION

The 200-µm-wide LOBARs and their comprising ladder filter were fabricated with a process described in [19]. The optical and SEM of a standalone resonator and the filter are shown in Fig. 6 and 7.

The measured admittance response of the series and shunt LOBARs are shown in Fig. 8. Multiple equally-spaced modes are successfully excited and harnessed by the transducers. The series resonances of the series resonators roughly align with the parallel resonances of the shunt resonators over the interested frequency range. The LOBARs have achieved Qs around 2000 and k_t^2 no smaller than 1% for 16 tones (14th -order mode to 50th-order mode, Fig. 9). The measured k_t^2 is 70% of the simulated values due to the existence of parasitic capacitances caused by the probing structures. The highest Q of 3633 is obtained for the 50th-order mode, while the highest k_t^2 of 2.02% is obtained for the 26th-order mode. The highest FoM of 39.9 is

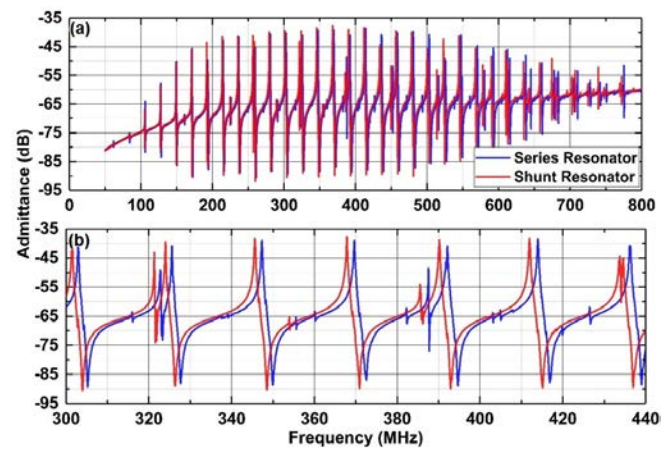


Fig. 8. Measured (a) wide-band and (b) zoomed-in admittance responses of the series and shunt resonators used in the ladder filter.

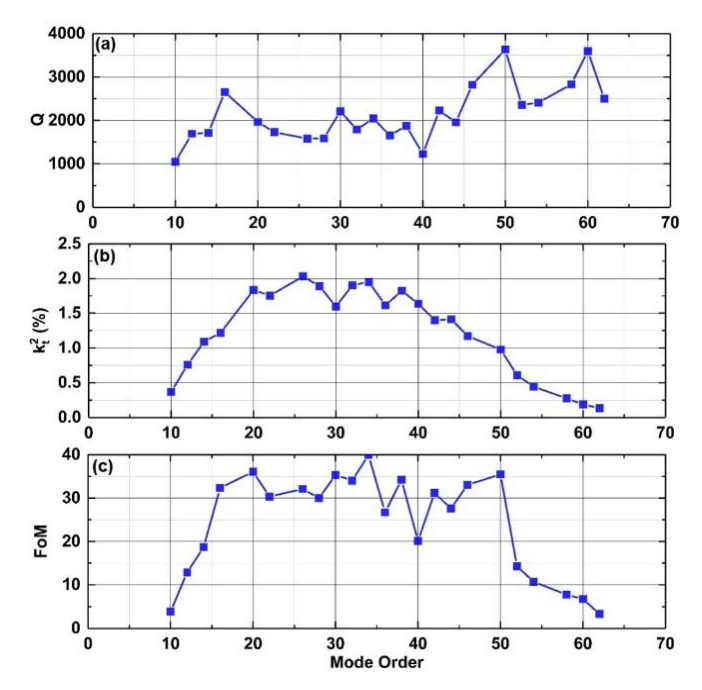


Fig. 9. Q, k_t^2 and FoM of each order extracted from the measurements done in dry air. The mode order is determined from the resonant frequency of each tone.

obtained for the 30th-order mode. A total capacitance (including static and parasitic capacitances) of 260 fF is measured. The *Q*s are among the highest ever reported in LiNbO₃ resonators, and the FoM are among the highest demonstrated in overmoded resonators.

The S-parameters of the fabricated filter were also measured with a network analyzer. The measurement was performed at 50 Ω system, and the port impedance was transformed to 3 $k\Omega$ in Advanced Design System for matching both input and output ports. The measured IL is shown in Fig. 10. The implemented periodic filter is centered at 370 MHz with a spectral spacing of 22 MHz. A low IL (around 2 dB), and FBWs around 0.6% (sparsification ratio around between 7 and 15) have been obtained, while an out-of-band rejection around 25 dB has been achieved for more than 14 bands. A minimum IL of 1.55 dB is obtained for the $24^{\text{th}}\text{-}\text{-}\text{order}$ mode. The highest FBW of 0.64 is

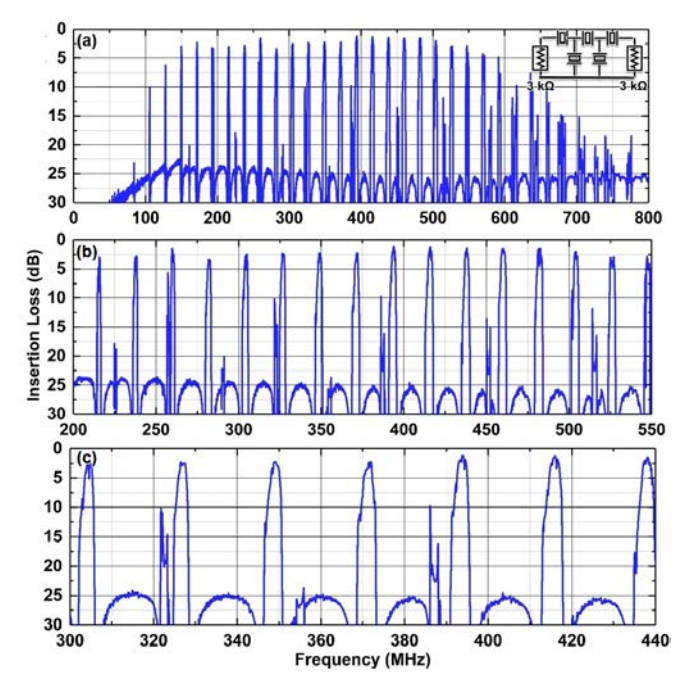


Fig. 10. Measured IL of the filter with periodic passbands. The measurements were done in dry air.

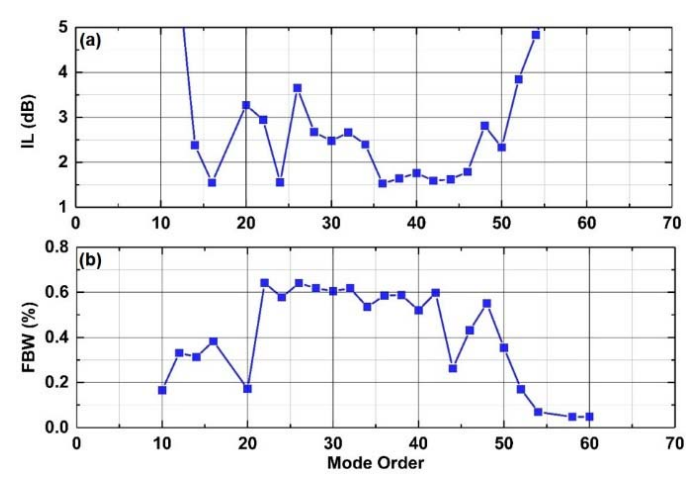


Fig. 11. Measured IL and 3-dB BW of different order passbands of the filter. The measurements were done in dry air.

obtained for the 22th-order mode. The key parameters of different passbands are shown in Fig. 11.

IV. ONCLUSION

This work demonstrates a passive low-IL RF filter with periodic passbands for SFT spectrum sensing based on LiNbO₃ LOBARs. The filter with periodic passbands was designed with LOBARs in the ladder topology. Resonators and filters were fabricated to validate our theory. The standalone LOBARs shows high k_i^2 larger than 1.5% and FoM more than 30 for over 10 tones, both among the highest demonstrated in overmoded resonators. The implemented periodic filter is centered at 370 MHz with a spectral spacing of 22 MHz. Low IL (around 2 dB in air, 1.5 dB in vacuum), and FBWs around 0.6% (sparsification ratio between 7 and 15) have been obtained, while an out-of-band rejection around 25 dB has been achieved for more than

14 bands. The great performance of this demonstration will serve to enable future SFT-based spectrum sensing.

REFERENCES

- F. C. Commission, "Second Memorandum opinion and Order (FCC 10-174)," US Govt. Print. Off. Washington, DC, vol. 23, 2010.
- [2] J. Mitola and G. Q. Maguire, "Cognitive radio: making software radios more personal," *IEEE Pers. Commun.*, vol. 6, no. 4, pp. 13–18, 1999.
- [3] M. Mishali and Y. C. Eldar, "Wideband spectrum sensing at sub-Nyquist rates [applications corner]," *IEEE Signal Process. Mag.*, vol. 28, no. 4, pp. 102–135, 2011.
- [4] U. Analog Devices, Norwood, MA, "12-Bit, 2.6 GSPS/2.5 GSPS/2.0 GSPS, 1.3 V/2.5 V Analog-to-Digital Converter AD9625 Data Sheet."
- [5] H. Hassanieh, L. Shi, O. Abari, E. Hamed, and D. Katabi, "Ghz-wide sensing and decoding using the sparse Fourier transform," in *INFOCOM*, 2014 Proceedings IEEE, 2014, pp. 2256–2264.
- [6] H. Hassanieh, P. Indyk, D. Katabi, and E. Price, "Simple and practical algorithm for sparse Fourier transform," in *Proceedings of the twenty-third annual ACM-SIAM symposium on Discrete Algorithms*, 2012, pp. 1183–1194.
- [7] R. C. Ruby, P. Bradley, Y. Oshmyansky, A. Chien, and J. D. I. Larson, "Thin film bulk wave acoustic resonators (FBAR) for wireless applications," 2001 IEEE Ultrason. Symp. Proceedings. An Int. Symp. (Cat. No.01CH37263), vol. 1, 2001.
- [8] P. V Wright, "A review of SAW resonator filter technology," in Ultrasonics Symposium, 1992, pp. 29–38.
- [9] G. Piazza, P. J. Stephanou, and A. P. Pisano, "Single-chip multiple-frequency ALN MEMS filters based on contour-mode piezoelectric resonators," *J. Microelectromechanical Syst.*, vol. 16, pp. 319–328, 2007.
- [10] S. Gong and G. Piazza, "Multi-frequency wideband RF filters using high electromechanical coupling laterally vibrating lithium niobate MEMS resonators," *Proc. IEEE Int. Conf. Micro Electro Mech. Syst.*, vol. 23, no. 5, pp. 785–788, 2013.
- [11] S. Gong, N. Kuo and G. Piazza, "GHz AlN lateral overmoded bulk acoustic wave resonators with a f · Q of 1.17 × 10¹³," 2011 Joint Conference of the IEEE International Frequency Control and the European Frequency and Time Forum (FCS) Proceedings, San Francisco, CA, USA, 2011, pp. 1-5.
- [12] B. P. Sorokin, G. M. Kvashnin, A. P. Volkov, V. S. Bormashov, V. V. Aksenenkov, M. S. Kuznetsov, G. I. Gordeev, and A. V. Telichko, "AlN/single crystalline diamond piezoelectric structure as a high overtone bulk acoustic resonator," *Appl. Phys. Lett.*, vol. 102, no. 11, p. 113507, 2013.
- [13] M. Pijolat, A. Reinhardt, E. Defay, C. Deguet, D. Mercier, M. Aid, J. S. Moulet, B. Ghyselen, D. Gachon, and S. Ballandras, "Large Qxf product for HBAR using Smart CutTM transfer of LiNbO 3 thin layers onto LiNbO 3 substrate," in *Ultrasonics Symposium*, 2008, pp. 201–204.
- [14] M. Ziaei-Moayyed, S. D. Habermehl, D. W. Branch, P. J. Clews, and R. H. Olsson, "Silicon carbide lateral overtone bulk acoustic resonator with ultrahigh quality factor," in *Micro Electro Mechanical Systems (MEMS)*, 2011 IEEE 24th International Conference on, 2011, pp. 788–792.
- [15] N.-K. Kuo, S. Gong, J. Hartman, J. Kelliher, W. Miller, J. Parke, S. V. Krishnaswamy, J. D. Adam, and G. Piazza, "Micromachined sapphire GHz lateral overtone bulk acoustic resonators transduced by aluminum nitride," in *Micro Electro Mechanical Systems (MEMS)*, 2012 IEEE 25th International Conference on, 2012, no. February, pp. 27–30.
- [16] R. Lu, T. Manzaneque, Y. Yang, A. Kourani, and S. Gong, "Lithium niobate lateral overtone resonators for low power frequency-hopping applications," in *Proceedings of the IEEE International Conference on Micro Electro Mechanical Systems (MEMS)*, 2018, vol. 2018–Janua.
- [17] R. Lu, T. Manzaneque, Y. Yang, and S. Gong, "Exploiting parallelism in resonators for large voltage gain in low power wake up radio front ends," in *Proceedings of the IEEE International Conference on Micro Electro Mechanical Systems (MEMS)*, 2018, pp. 747–750.
- [18] Y.-H. Song, R. Lu, and S. Gong, "Analysis and removal of spurious response in SH0 lithium niobate MEMS resonators," *IEEE Trans. Electron Devices*, vol. 63, no. 5, pp. 2066–2073, May 2016.
- [19] Y. Yang, R. Lu, T. Manzaneque, and S. Gong, "Towards Ka Band Acoustics: Lithium Niobate Asymmetrical Mode Piezoelectric MEMS Resonators," in *IEEE International Frequency Control Symposium* (IFCS), 2018.